International Journal of Nanomedicine

Dovepress
open access to scientific and medical research

Open Access Full Text Article

ORIGINAL RESEARCH

Development of a new carbon nanotube–alginate–hydroxyapatite tricomponent composite scaffold for application in bone tissue engineering

Rajendiran Rajesh
Y Dominic Ravichandran

Organic Chemistry Division, School of Advanced Sciences, VIT University, Vellore, India

Abstract: In recent times, tricomponent scaffolds prepared from naturally occurring polysaccharides, hydroxyapatite, and reinforcing materials have been gaining increased attention in the field of bone tissue engineering. In the current work, a tricomponent scaffold with an oxidized multiwalled carbon nanotube (fMWCNT)–alginate–hydroxyapatite with the required porosity was prepared for the first time by a freeze-drying method and characterized using analytical techniques. The hydroxyapatite for the scaffold was isolated from chicken bones by thermal calcination at 800°C. The Fourier transform infrared spectra and X-ray diffraction data confirmed ionic interactions and formation of the fMWCNT–alginate–hydroxyapatite scaffold. Interconnected porosity with a pore size of 130–170 μm was evident from field emission scanning electron microscopy. The total porosity calculated using the liquid displacement method was found to be 93.85%. In vitro biocompatibility and cell proliferation on the scaffold was checked using an MG-63 cell line by 3-(4,5-dimethylthiazol-2-yl)-2,5-diphenyltetrazolium bromide assay and cell attachment by Hoechst stain assay. In vitro studies showed better cell proliferation, cell differentiation, and cell attachment on the prepared scaffold. These results indicate that this scaffold could be a promising candidate for bone tissue engineering.

Keywords: chicken bone, hydroxyapatite, alginate, tissue engineering

Introduction

Bone is a live, dynamic, and highly vascularized tissue with a unique capacity to heal and remodel itself without scarring. The complex architecture of bone, composed of organic and inorganic materials along with water, throws open a new area of research to develop tricomponent scaffolds that can mimic bone. The organic materials include an extracellular matrix (ECM) composed of collagen, osteocalcin, osteonectin, osteoadherin, fibronectin, thrombospondin, proteoglycan, and glycosaminoglycan. The major important inorganic mineral in bone is hydroxyapatite (HAP), in addition to a few minor minerals including magnesium, potassium, fluoride, phosphate, and citrate.[1–3] Bone defects and trauma are some of the problems experienced in the middle-aged population.[4] These defects are treated by metal implants or traditional bone grafting techniques, including autografts and allografts. The major problem with metal implants is that they are nondegradable. Hence, the procedure requires secondary surgery. Moreover, metal implants cause stress and release toxic ions, resulting in infection. Further, bone grafting has some limitations, including restriction of the donor site, additional surgery, cost, and unwanted transmission of disease.[2,5–8] Hence, alternative materials need to be developed to overcome these drawbacks.

Correspondence: Y Dominic Ravichandran
Organic Chemistry Division, School of Advanced Sciences, VIT University, Vellore 632014, Tamiln Nadu, India
Email ydominic64@yahoo.co.in

submit your manuscript | www.dovepress.com
Dovepress
http://dx.doi.org/10.2147/IJN.S79971

Bone tissue engineering is a complex and dynamic process that starts with migration and moves on to recruitment of osteoprogenitor cells, followed by their proliferation and differentiation, and formation of matrix, along with remodeling of bone.[4] In tissue engineering, a three-dimensional scaffold matrix is developed to support cells, promoting their differentiation and proliferation, and acting as a carrier to transfer cells and bioactive materials to the defective site for formation of new tissue.[9,10]

The natural ECM brings cells together and controls tissue structure, regulates the function of cells, allows diffusion of nutrients and metabolites, and facilitates tissue development.[10,11] This has created a need to find biocompatible materials with the ability to mimic the natural ECM and allow tissue regeneration. Natural polysaccharides can mimic the ECM because of their similar bioactivity to ECM.[9,10] They can also avoid stimulation of chronic inflammation or immunological reactions and toxicity, which is often found with synthetic polymers.[9,12]

Alginate, a polysaccharide extracted from seaweed and composed of 1,4-linked β-D-mannuronic acid and α-L-guluronic acid residues, has the ability to form a gel at room temperature when cross-linked with divalent cations such as calcium. Further, alginate has several biomedical applications, including cell and drug delivery, dental impressions, wound dressing, and bone tissue engineering.[13–16]

HAP is a well established material in bone tissue engineering because of its biocompatibility and osteoconductivity. There are many sources of HAP.[3,7,17,18] Chemically synthesized HAP is not preferred because of its limited biocompatibility, osteoconduction, and bioresorption. Hence, isolation of natural carbonated HAP from bones is preferred to chemical synthesis.[6,19] The major disadvantage of HAP in bone engineering is its poor mechanical strength and brittleness, which make it unfit for major load-bearing applications.[7] Hence, reinforcing materials are incorporated to increase mechanical strength and to improve the load-bearing capacity. Carbon nanotubes (CNTs) are an excellent reinforcement material owing to their enhanced toughness and flexural strength. Incorporation of CNTs in the scaffold as a reinforcing material improves the strength considerably. Further, CNTs enable excellent cell proliferation, and have several biomedical applications, including cancer therapy, treatment of central nervous system disorders, tissue engineering, and biosensors. There are a number of reports of CNTs being toxic in many cell lines, but this can be overcome by functionalization.[6,20–23] Hence, we developed a novel CNT–alginate–HAP scaffold and investigated cell proliferation and cell attachment for the first time.

Materials and methods

Materials

HAP was isolated from chicken bones (purchased from a local slaughter house) using the thermal calcination method. Multiwalled CNTs (MWCNTs, outer diameter <8 nm, length 10–30 μm) were purchased from cheap tubes.com (Cambridgeport, VT, USA). The MG-63 cell line was sourced from the National Center for Cell Science (Pune, India). Sodium alginate, 3-(4,5-dimethylthiazol-2-yl)-2,5-diphenyltetrazolium bromide (MTT), and bisbenzimide (Hoechst 33342) stain were purchased from Sigma-Aldrich (St Louis, MO, USA). Dulbecco's Modified Eagle's Medium was sourced from HiMedia Laboratories (Mumbai, India). Sodium phosphate buffer, NaCl, and KCl were obtained from Merck (Whitehouse Station, TX, USA). NaOH, conc.HNO_3 and conc.H_2SO_4 (analytical grade) were purchased from S D Fine-Chem (Mumbai, India).

Isolation of HAP from chicken bone

HAP was isolated by thermal calcination as reported previously by our group.[3] The chicken bones were washed with concentrated NaOH solution, then rinsed with water to remove traces of meat, skin, and other impurities present on the surface of the bones. The bones were then dried in a hot air oven at 100°C and grained into small pieces. Pretreated chicken bones were subjected to thermal calcination at 800°C, with 20 hours of holding time in an electrical muffle furnace.

Oxidation of MWCNTs

MWCNTs were oxidized using a modification of the procedure reported by An et al.[24] The MWCNTs were sonicated in a 3:1 mixture of conc.HNO_3 and conc.H_2SO_4 for 20 minutes, then refluxed for 3 hours. The oxidized (f)MWCNTs were centrifuged, washed with distilled water, and then dried in an oven at 100°C overnight.

Preparation of fMWCNT–alginate–HAP scaffold

First, 1.74 g of alginate were dissolved in 100 mL of double-distilled water. Next, 60 mg of fMWCNT were dispersed in distilled water by sonication and added dropwise to the alginate solution, followed by stirring for 3 hours; 4.2 g of isolated HAP suspended in 50 mL of distilled water were then added slowly to the fMWCNT–alginate solution, and the resulting solution was stirred for 24 hours. Finally, 4 g of the resulting black-colored mixture was transferred to 12-well plates, frozen at −80°C, and lyophilized using a freeze-drier to form the scaffold.

Characterization

The thermal stability of the scaffold was studied using thermogravimetric analysis (SDTQ 600, TA Instruments, New Castle, DE, USA) with scan range of 30°C–800°C at a constant heating rate of 10°C per minute in a nitrogen atmosphere. The vibrational frequency of the samples was studied by Fourier transform infrared (FTIR) spectroscopy (FTIR4100, Jasco, Tokyo, Japan) by recording the spectrum in the range of 4,000–500 cm^{-1} with KBr. The phase and crystallinity of the samples were examined by X-ray diffraction (D8 Advance spectrophotometer, Bruker, Karlsruhe, Germany) at room temperature using Cu Kα as the radiation source, with a wavelength of 1.504 Å over an angle range of 10°–80°, along with a step size of 0.02° and a scan speed of 0.5° per minute. The resulting X-ray diffraction profile for the isolated HAP was compared with the standard Joint Committee on Powder Diffraction Standards cards available in the system software. Further, the morphology of the tricomponent scaffold was studied by field emission scanning electron microscopy (FESEM, Supra 55, Carl Zeiss, Oberkochen, Germany).

Porosity measurements

Porosity is an important property for cell proliferation. The total porosity of the scaffold was determined by the liquid displacement method. First, the volume of dry ethanol and dry weight of the scaffold were measured. The scaffold was then immersed in dry ethanol for 48 hours. After 48 hours, the scaffold was removed from the ethanol and the weight of the scaffold was measured. The total porosity was calculated using the equation:

$$\text{Porosity} = (W_1 - W_3)/(W_2 - W_3)$$

where W_1 is the initial weight of the scaffold, W_2 is the sum of the weights of ethanol and the submerged scaffold, and W_3 is the weight of ethanol after removal of the scaffold.[25]

Cell proliferation assay

MG-63 cells were plated in 96-well plates at a concentration of 1×10^5 cells/well. After 24 hours, the cells were washed twice with 100 µL of serum-free medium and starved for an hour at 37°C. Next, the cells were seeded with the scaffold material which was previously sterilized with 75% alcohol followed by 100% alcohol. At the end of treatment, the medium was aspirated and serum-free medium containing MTT 0.5 mg/mL was added and incubated for 4 hours at 37°C in a CO_2 incubator.

The medium containing MTT was then discarded and the cells were washed in 200 µL of phosphate-buffered saline. The formazan crystals formed were then dissolved by adding 100 µL of dimethyl sulfoxide, and this was mixed thoroughly by pipetting up and down. Absorbance of the purple-blue formazan dye was measured in a microplate reader (Model 680, Bio-Rad Laboratories, Hercules, CA, USA) at 570 nm. Cytotoxicity was determined using GraphPad Prism version 5 software (GraphPad Software, La Jolla, CA, USA).

Hoechst stain assay for cell attachment

Hoechst 33342 DNA staining is used to identify cell attachment and growth on scaffold material.[25] For this, the ethanol-sterilized scaffold material was placed in a cell culture plate, seeded with MG-63 cells, and incubated. After 4 days of culture, the medium was removed from the wells and washed in phosphate-buffered saline. The cells were stained with 0.5 mL of Hoechst 33342 solution (3.5 µg/mL in phosphate-buffered saline) and incubated for 30 minutes at 37°C. After 30 minutes, the Hoechst-stained cells were visualized and photographed using an Olympus (Tokyo, Japan) microscope (version 6.0) with a Carl Zeiss lens.[23]

Acridine orange stain assay for cell attachment

Acridine orange is used to identify both viable and apoptotic cells on scaffold materials.[26] For this, ethanol-sterilized scaffold material was placed in a cell culture plate and seeded with MG-63 cells and incubated. After 4 days of culture, the medium was removed from the wells and washed with phosphate-buffered saline. The cells were stained with 200 µL of dye mixture (100 µL/mg acridine orange in distilled water). The suspension was immediately examined and photographed using the Olympus microscope with the Carl Zeiss lens.[23]

Alkaline phosphatase assay

To determine alkaline phosphatase (ALP) activity, the cells were cultured as per the cytotoxicity analysis after incubation with the scaffold for 2 and 4 days. The cells were treated with 10 µL (100 mmol/L) of p-nitrophenyl phosphate and incubated for 30 minutes at 37°C in a CO_2 incubator. ALP expressed by cells hydrolyzes p-nitrophenyl phosphate to *p*-nitrophenol and inorganic phosphate.[27] Under alkaline conditions, the *p*-nitrophenol is converted to a yellow product, and its absorbance is measured spectrophotometrically at 405 nm. These determinations were performed using three replicates each time.

Compressive strength

The compressive strength of the freeze-dried scaffold was determined using a universal testing machine. The tests were performed using an H5KS system (Tinius Olsen, Salfords, UK). A 5,000 N load cell with standard grips of crosshead speed of 0.5 mm per minute was used for the compression measurements.

Statistical analysis

Statistical analysis of the MTT assay, ALP assay, and compressive strength were performed using GraphPad Prism version 5 software.

Results and discussion

Material selection and ratio

In this study, three raw materials, ie, alginate, HAP, and fMWCNT, were used to prepare a scaffold mimicking the role of the ECM in bone. Since natural bone is composed of 70% inorganic mineral (HAP) and 30% organic materials (collagen), 70% of HAP, 29% of alginate, and 1% fMWCNT were used for preparation of the scaffold. In order to remove the toxicity of pristine CNT, CNT was functionalized. The acid-functionalized CNT showed better dispersion in aqueous solution and more interaction with cells. Further, the hydrophilic nature of alginate facilitated homogeneous distribution of the aqueous solution containing HAP and fMWCNT. This enhanced cell adhesion, proliferation, and differentiation.[6,28]

Thermal stability

The thermal stability of the fMWCNT–alginate–HAP scaffold was determined by thermogravimetric analysis. A comparison of weight loss from the fMWCNT–alginate–HAP scaffold and that of the raw materials is shown in Figure 1. The 3% weight loss observed at 30°C–135°C in the scaffold was due to removal of adsorbed water molecules. The 37.5% weight loss observed at 202°C–441°C could be attributed to decomposition of alginate into carbonaceous material. The thermal stability of fMWCNT and HAP is evident in Figure 1. The absence of any significant weight loss in the fMWCNT–alginate–HAP scaffold as compared with alginate above 500°C indicates the increase in thermal stability and strong interaction of alginate with thermally stable fMWCNT and HAP.[6,7,29]

FTIR analysis

FTIR spectra for the alginate, fMWCNT, HAP, and fMWCNT–alginate–HAP scaffold are shown in Figure 2. All

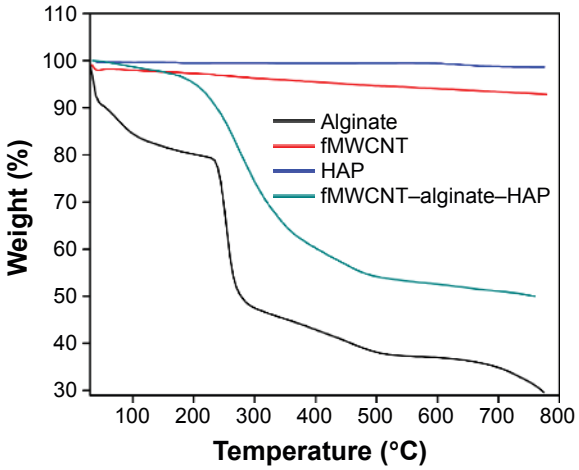

Figure 1 Thermogravimetric images of fMWCNT–alginate–HAP composite scaffold.
Abbreviations: fMWCNT, oxidized multiwalled carbon nanotube; HAP, hydroxyapatite.

the characteristic bands expected of HAP were observed in the FTIR spectra; $\nu_3 PO_4^{3-}$ showing symmetrical triply degenerate bending at 1,049 cm^{-1}, $\nu_1 PO_4^{3-}$ symmetrical nondegenerate stretching at 966 cm^{-1}, $\nu_4 PO_4^{3-}$ antisymmetric bending at 570 cm^{-1}, $\nu_2 PO_4^{3-}$ antisymmetric doubly degenerate stretching at 476 cm^{-1}, $\nu_3 CO_3^{2-}$ at 1,460 cm^{-1}, $\nu_2 CO_3^{2-}$ at 881 cm^{-1}, and OH^- at 3,570 and 634 cm^{-1}.[3,6] For alginate, the FTIR spectrum showed the following characteristic bands, as reported in

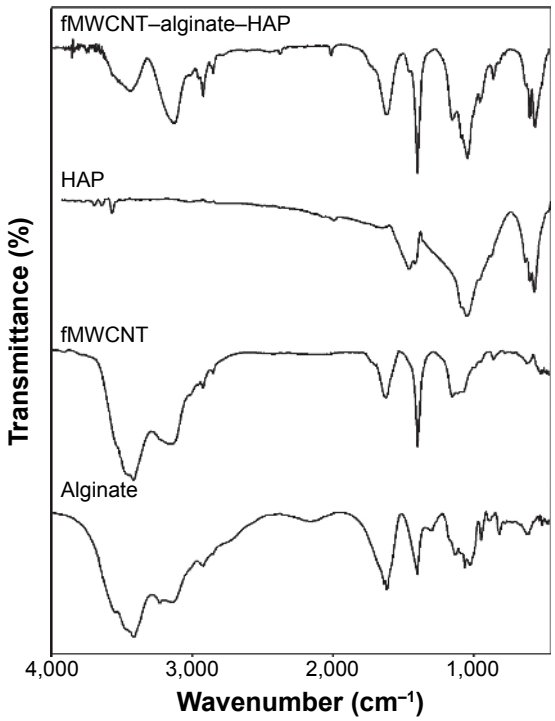

Figure 2 Fourier transform infrared spectra of alginate, fMWCNT, HAP, and fMWCNT–alginate–HAP composite scaffold.
Abbreviations: fMWCNT, oxidized multiwalled carbon nanotube; HAP, hydroxyapatite.

the literature; OH^- stretching at 3,414 cm^{-1}, C-H stretching vibrations at 2,924 cm^{-1}, symmetrical COO^- stretching at 1,612 cm^{-1}, asymmetrical COO^- stretching at 1,402 cm^{-1}, and C-O-C (saccharide structure) stretching at 1,064 cm^{-1}.[30,31] Further, the functionalization of MWCNTs was confirmed by the OH^- stretching vibration at 3,500 cm^{-1}, carbon skeleton at 3,138 cm^{-1}, carbonyl (COOH) at 1,638 cm^{-1}, C-C stretching vibration at 1,402 cm^{-1}, and C-O stretching vibration at 1,044 cm^{-1}.[6,7,32] The FTIR spectrum for the fMWCNT–alginate–HAP scaffold showed characteristic peaks for all its components, ie, alginate, HAP, and fMWCNT, with a slight shift in wave numbers. The peaks corresponding to HAP shifted from 881 cm^{-1} to 862 cm^{-1} and from 966 cm^{-1} to 958 cm^{-1}, and the peak corresponding to alginate shifted from 1,612 cm^{-1} to 1,618 cm^{-1}. These observed peak shifts may be attributed to the ionic interactions of alginate with fMWCNT and HAP.[6,7,33] The stretching vibrations of phosphate at 1,049 cm^{-1} in pure HAP shifted to 1,045 cm^{-1}. This might be due to the strong hydrogen bonding between the individual components present in the fMWCNT–alginate–HAP scaffold.[34] These results confirm the presence of all components in the scaffold and that formation of the composite was due to ionic interactions and hydrogen bonding.

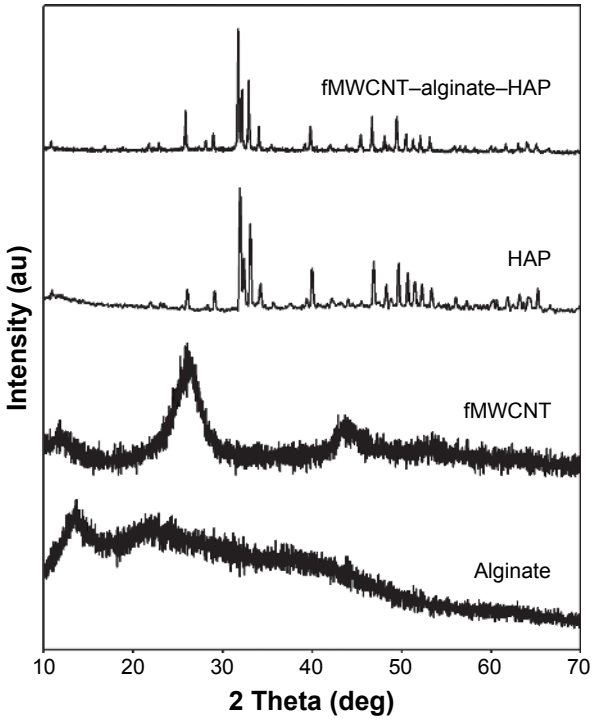

Figure 3 X-ray diffraction patterns of alginate, fMWCNT, HAP, and fMWCNT–alginate–HAP composite scaffold.
Abbreviations: fMWCNT, oxidized multiwalled carbon nanotube; HAP, hydroxyapatite.

X-ray diffraction analysis

The X-ray diffraction pattern for alginate, fMWCNT, HAP, and the fMWCNT–alginate–HAP scaffold are shown in Figure 3. The X-ray diffraction values for the isolated HAP were found to be in good conformity with those for standard HAP (Joint Committee on Powder Diffraction Standards card 09-0432/1996) as reported earlier.[3] Two major peaks at 13.57° and 22.75° for alginate and one peak at 26.05° for fMWCNT were observed. The broadening in the diffraction spectrum for alginate and fMWCNT was due to the amorphous nature of alginate and fMWCNT. All the characteristic peaks for the raw materials were observed in the scaffold, with a slight shift in 2θ values (31.95° to 31.74°, 33.09° to 32.92°, 39.90° to 39.80°, and 49.65° to 49.47°) and reduced intensity of the peaks corresponding to alginate and fMWCNT. Moreover, the composite scaffold had a less crystalline nature than the raw HAP. The slight amorphous nature and decreased crystalline nature were attributed to the amorphous character induced by alginate. The slight shift in 2θ values of the scaffold was attributed to the strong ionic interactions between the components.[6,25]

FESEM analysis

FESEM analysis is an important technique for identifying the morphology and porous nature of a scaffold material. The FESEM images of the isolated HAP and composite scaffold are shown in Figure 4. FESEM images of the isolated HAP confirmed the crystalline nature with a crystal size of 300–400 nm and those of the fMWCNT–alginate–HAP scaffold confirmed the interconnected pore structure, with a pore size of 130–170 μm. The uniform distribution of HAP and fMWCNT in alginate can be observed in Figure 4B and C. This could be due to the electrically charged nature of the alginate.[4,25]

Porosity measurement

Porosity of at least 90% is required for formation of bone tissue, and increased porosity is crucial for cell growth. Porosity allows migration and proliferation of osteoblasts and mesenchymal cells, and aids in vascularization, thereby providing temporary mechanical function and delivering genes and proteins.[25] The overall porosity of the prepared fMWCNT–alginate–HAP scaffold was determined by the liquid displacement method, and was found to be 93.85%, which meets the requirements for cell migration and tissue growth.[35]

Cytotoxicity study

The cell proliferation and biocompatibility of the scaffold were investigated in an MG-63 cell line using the MTT

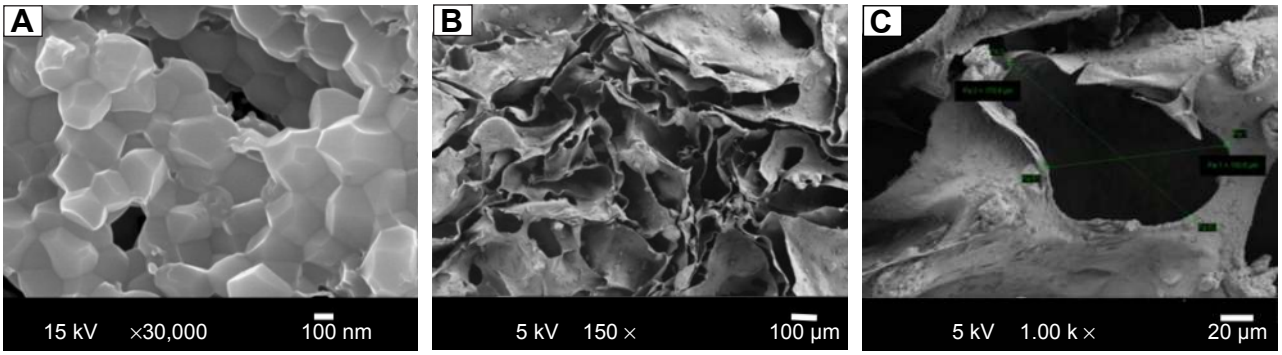

Figure 4 Field emission scanning electron micrographs of HAP (**A**) and fMWCNT–alginate–HAP composite scaffold (**B**, **C**).
Abbreviations: fMWCNT, oxidized multiwalled carbon nanotube; HAP, hydroxyapatite.

assay, and the results are shown in Figure 5. The scaffold was found to be nontoxic to the osteoblast-like MG-63 cell line. However, cell proliferation in the scaffold was lower when compared with the control for the first 2 days, but increased on days 3 and 4, by which time it almost matched that of the control. There are reports that cells seeded onto scaffolds with large pores undergo faster migration, and that a larger surface area and pore size enable greater cell proliferation. This might be due to the favorable spatial arrangement of cells. The surface area and pore size (130–170 µm) of fMWCNT–alginate–HAP was sufficiently large to allow cell proliferation, and favorable spatial arrangement of cells increases cell proliferation and biocompatibility.[25,28] The interconnected pore structure of fMWCNT–alginate–HAP facilitated cell migration to internal pores and flow of nutrients and metabolic waste, and also enhanced communication of cells in different pores during cell culture.[36] The biocompatibility of the scaffold in the MG-63 cell line indicates that the scaffold material can be used for bone tissue engineering.

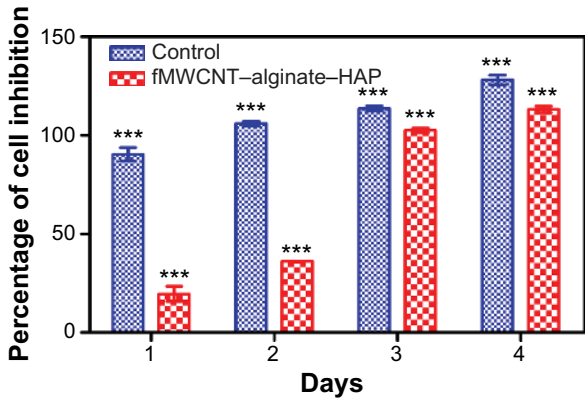

Figure 5 In vitro biocompatibility and cell proliferation of fMWCNT–alginate–HAP composite scaffold by MTT assay as a function of days.
Notes: Values are expressed as the mean ± standard deviation (n=3). Statistical analysis was performed using two-way analysis of variance (***$P<0.001$).
Abbreviations: fMWCNT, oxidized multiwalled carbon nanotube; HAP, hydroxyapatite; MTT, 3-(4,5-dimethylthiazol-2-yl)-2,5-diphenyltetrazolium bromide.

Cell attachment study

Cell proliferation and distribution on the composite scaffold was viewed by fluorescence microscopy after staining with acridine orange and Hoechst 3342. Fluorescent Hoechst 33342 DNA staining is commonly used to visualize nuclei and mitochondria in which the cell nuclei appear blue after staining,[25,28] whereas acridine orange can bind with double-stranded DNA of live cells and emits green fluorescence. Viable cells have uniform bright green nuclei with an organized structure.[26] Optical microscopy images of blue-colored Hoechst-stained (Figure 6A and B) and green-colored acridine orange-stained (Figure 6C and D) scaffolds clearly confirmed the higher density cell attachment on the composite scaffold. The cells were present both individually and in aggregated form. The hydroxyl group present in alginate can easily bind with cell proteins for better cell adhesion. Moreover, the smaller size of MG-63 cells can easily adhere and migrate within the interconnected porous of large-sized pores (130–170 µm) of the scaffold.[37]

Cell differentiation

ALP activity is the most common indicator of expression of osteoblastic differentiation.[38,39] The skeletal isoform of ALP is a glycoprotein found on the cell membrane of osteoblasts and plays an important role in mineralization of the bone matrix.[40] ALP activity of cells in the fMWCNT–alginate–HAP scaffold was measured on days 2 and 4, and the results are shown in Figure 7. The ALP activity in cells on the scaffold increased with increasing number of days. These results confirm that the prepared tricomponent scaffold enabled better cell differentiation.

Compressive strength

Tissue-engineered scaffolds should have enough mechanical strength to support regeneration of bone tissue and maintain

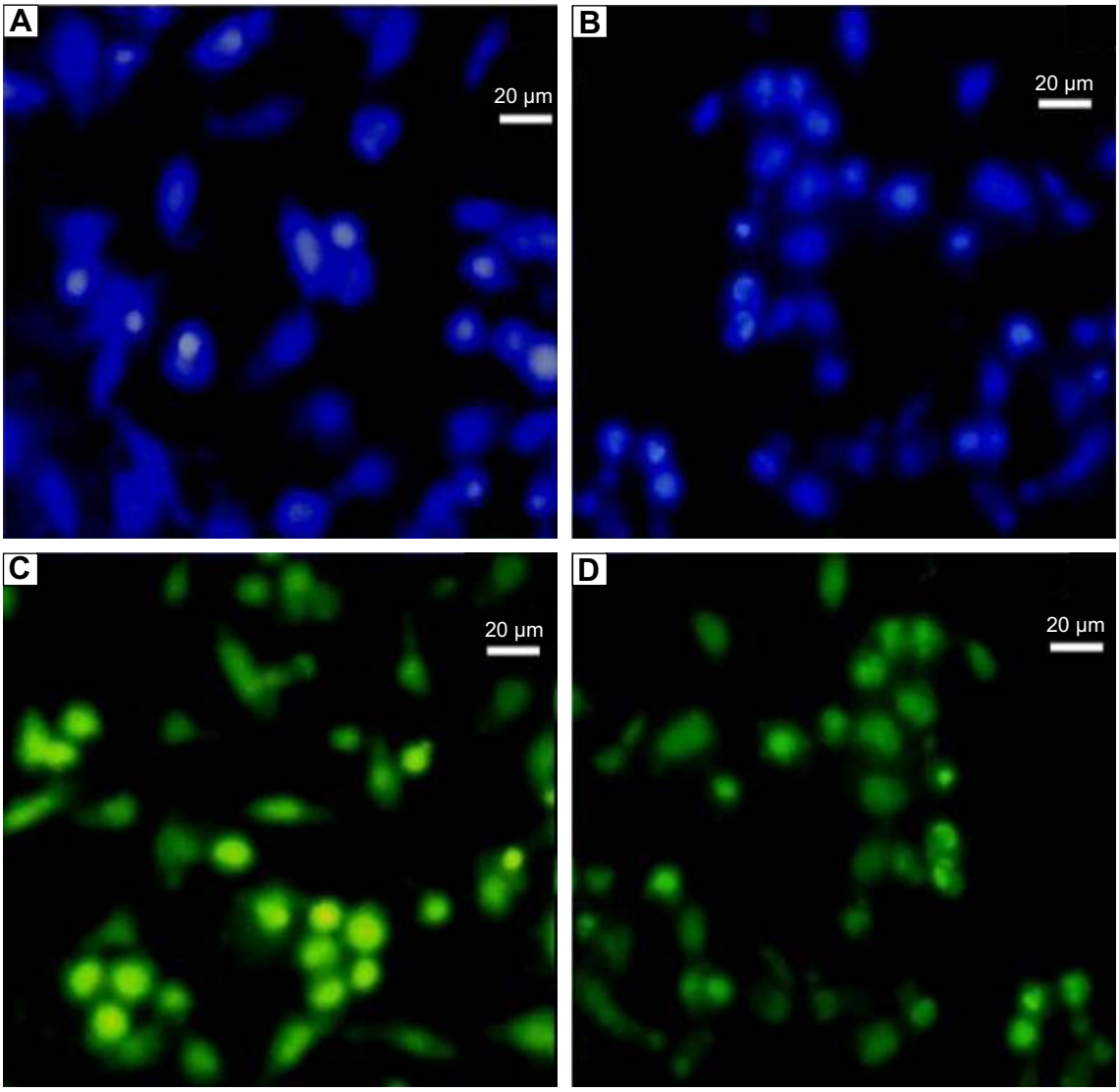

Figure 6 Optical microscopy images of Hoechst 3342-stained (**A**, **B**) and acridine orange-stained (**C**, **D**) cells grown on scaffold.

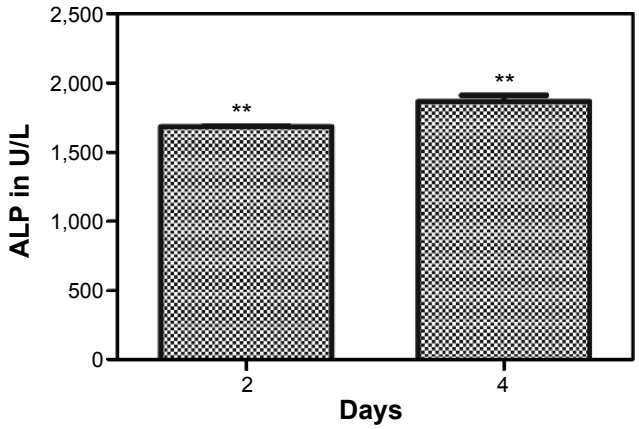

Figure 7 ALP assay of fMWCNT–alginate–HAP scaffolds on MG 63 cell line.
Notes: Values are expressed as the mean ± standard deviation (**$P<0.05$, n=3).
Abbreviations: ALP, alkaline phosphatase; fMWCNT, oxidized multiwalled carbon nanotube; HAP, hydroxyapatite.

sufficient integrity at the site of implantation during in vitro and in vivo cell growth. The major hurdle in the preparation of porous scaffolds is their lower mechanical strength.[41] In order to evaluate the mechanical strength of the freeze-dried scaffold, compressive strength was tested and the results are shown in Figure 8. The compressive strength was found to be 72.02±1.7 kPa ($P<0.001$, n=5) which is comparable with that of previously reported freeze-dried scaffolds.[42–44] The lower compressive strength was due to the higher porosity of the scaffold.

Conclusion

We have developed a novel fMWCNT–alginate–HAP scaffold using a freeze-drying method to mimic the properties

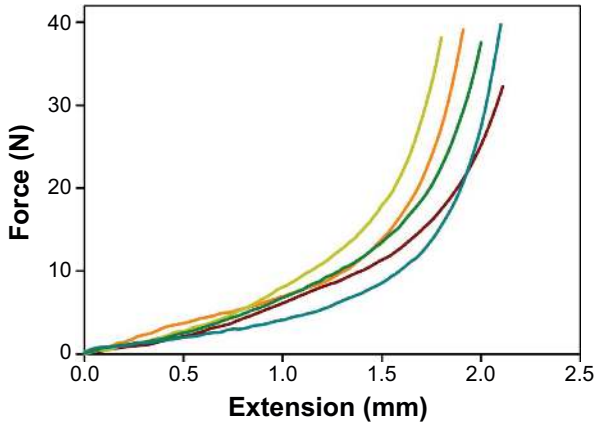

Figure 8 Scaffold images showing compressive strength.

of the ECM. The analytical results confirmed successful formation of the scaffold, with strong ionic and hydrogen bonding interactions. The porosity of the developed tricomponent scaffold was 93.85% and the interconnected pore size was 130–170 μm. The scaffold material showed improved compressive strength (72.02±1.7 kPa). The scaffold showed better biocompatibility, cell differentiation, and cell attachment in in vitro cytotoxicity on MG-63 cell. These results indicate that the prepared scaffold could be a potential candidate for applications in bone tissue engineering.

Acknowledgments

The authors gratefully acknowledge the management of VIT University, Vellore, India, for providing the facilities needed to carry out this work. RR gratefully acknowledges his RA fellowship from VIT University. The authors also acknowledge the powder X-ray diffraction facility at SAS, VIT University, jointly funded by Vellore Institute of Technology and Fund for Improvment of Science & Technology Infrastructure, Department of Science and Technology, New Delhi, India. Further, the authors thank the Pondicherry Center for Biological Sciences for the in vitro studies.

Disclosure

The authors report no conflicts of interest in this work.

References

1. Salgado AJ, Coutinho OP, Reis RL. Bone tissue engineering: state of the art and future trends. *Macromol Biosci.* 2004;4:743–765.
2. Eslaminejad MB, Bagheri F. Tissue engineering approach for reconstructing bone defects using mesenchymal stem cells. *Yakhteh Medical Journal*. 2009;11:263–272.
3. Rajesh R, Hariharasubramanian A, Ravichandran YD. Chicken bone as a bioresource for the bioceramic (hydroxyapatite). *Phosphorus Sulfur Silicon Relat Elem*. 2012;187:914–925.
4. Bose SM, Roy M, Bandyopadhyay A. Recent advances in bone tissue engineering scaffolds. *Trends Biotechnol.* 2012;30:546–554.
5. Venkatesan J, Kim SK. Stimulation of minerals by carbon nanotube grafted glucosamine in mouse mesenchymal stem cells for bone tissue engineering. *J Biomed Nanotechnol.* 2012;8:1–10.
6. Venkatesan J, Qian Z-J, Ryu BM, Kumar NA, Kim SK. Preparation and characterization of carbon nanotube-grafted-chitosan-natural hydroxyapatite composite for bone tissue engineering. *Carbohydr Polym.* 2011;83:569–577.
7. Rajesh R, Hariharasubramanian A, Senthilkumar N, Ravichandran YD. A biocompatible and load bearing composite of multiwalled carbon nanotubes chitosan and natural hydroxyapatite derived from the chicken bones wasted in the slaughter houses. *Int J Pharm Pharm Sci.* 2012;4:716–720.
8. Burg KJ, Porter S, Kellam JF. Biomaterial developments for bone tissue engineering. *Biomaterials*. 2000;21:2347–2359.
9. Mano JF, Silva GA, Azevedo HS, et al. Natural origin biodegradable systems in tissue engineering and regenerative medicine: present status and some moving trends. *J R Soc Interface.* 2007;4:999–1030.
10. Tonelli FM, Santos AK, Gomes KN, et al. Carbon nanotube interaction with extracellular matrix proteins producing scaffolds for tissue engineering. *Int J Nanomedicine.* 2012;7:45111–4529.
11. Lee KY, Mooney DJ. Hydrogels for tissue engineering. *Chem Rev.* 2001;101:1869–1879.
12. Grandfield K, Sun F, Fitzpatrick M, Cheong M, Zhitomirsky I. Electrophoretic deposition of polymer-carbon nanotube-hydroxyapatite composites. *Surf Coat Technol.* 2009;203:1481–1487.
13. Bouchadir KH, Lee KY, Alsberg E, Damm KL, Anderson KW, Mooney DJ. Degradation of partially oxidized alginate and its potential application for tissue engineering. *Biotechnol Prog.* 2001;17:945–950.
14. Wang L, Shelton RM, Cooper PR, Lawson M, Triffitt JT, Barralet JE. Evaluation of sodium alginate for bone marrow cell tissue engineering. *Biomaterials*. 2003;24:3475–3481.
15. Alsberg E, Anderson KW, Albeiruti A, Franceschi RT, Mooney DJ. Cell-interactive alginate hydrogels for bone tissue engineering. *J Dent Res.* 2001;80:2025–2029.
16. Fundueanu G, Nastruzzi C, Carpov A, Desbrieres J, Rinaudo M. Physico-chemical characterization of Ca-alginate microparticles produced with different methods. *Biomaterials.* 1999;20:1427–1435.
17. Rajesh R, Senthilkumar N, Hariharasubramanian A, Ravichandran YD. Review on hydroxyapatite-carbon nanotube composites and some of their applications. *Int J Pharm Pharm Sci.* 2012;4:23–27.
18. Rajesh R, Ravichandran YD, Raj NA, Senthilkumar N. Development of a biodegradable composite (hydroxyapatite-chitosan-coir pith) as a packing material. *Polym-Plast Technol.* 2014;53:1105–1110.
19. Barakat NA, Khalil KA, Sheikh FA, et al. Physiochemical characterizations of hydroxyapatite extracted from bovine bones by three different methods: extraction of biologically desirable Hap. *Mater Sci Eng C.* 2008;28:1381–1387.
20. Zhang Y, Bai Y, Yan B. Functionalized carbon nanotubes for potential medicinal applications. *Drug Discov Today.* 2010;15:428–435.
21. Zanello LP, Zhao B, Hu H, Haddon RC. Bone cell proliferation on carbon nanotubes. *Nano Lett.* 2006;6:562–567.
22. Hariharasubramanian A, Ravichandran YD, Rajesh R, Kumar KR, Kanagaraj M, Arumugam S. Covalent functionalization of single-walled carbon nanotubes with anthracene by green chemical approach and their temperature dependent magnetic and electrical conductivity studies. *Mater Chem Phys.* 2014;143:838–844.
23. Hariharasubramanian A, Ravichandran YD, Rajesh R, Rajkumari R, Selvan GK, Arumugam S. Functionalization of multi-walled carbon nanotubes with 6-aminobenzothiazole and their temperature-dependent magnetic studies. *Fuller Nanotub Car N.* 2014;22:874–886.
24. An JS, Nam BU, Tan SH, Hang SC. Study on the functionalization of multi-walled carbon nanotube with monoamine terminated poly(ethylene oxide). *Macromol Symp.* 2007;249–250:267–282.
25. Venkatesan J, Pallela R, Bhatnagar I, Kim SK. Chitosan-amylopectin/hydroxyapatite and chitosan-chondroitin sulphate/hydroxyapatite composite scaffolds for bone tissue engineering. *Int J Biol Macromol.* 2012;51:1033–1042.

26. Baskic D, Popovic S, Ristic P, Arsenijevic NN. Analysis of cycloheximide-induced apoptosis in human leukocytes: fluorescence microscopy using annexin V/propidium iodide versus acridin orange/ethidium bromide. *Cell Biol Int.* 2006;30:924–932.
27. Venkatesan J, Kim S-K. Stimulation of minerals by carbon nanotube grafted glucosamine in mouse mesenchymal stem cells for bone tissue engineering. *J Biomed Nanotechnol.* 2012;8:676–685.
28. Thein-Han WW, Misra RD. Biomimetic chitosan-nanohydroxyapatite composite scaffolds for bone tissue engineering. *Acta Biomater.* 2009;5:1182–1197.
29. Soares JP, Santos JE, Chierice GO, Cavalheiro ET. Thermal behavior of alginic acid and its sodium salt. *Ecletica Quimica.* 2004;29:53–56.
30. Wang L, Li Y, Li C. In situ processing and properties of nanostructured hydroxyapatite/alginate composite. *J Nanopart Res.* 2009;11:691–696.
31. Leal D, Matsuhiro B, Rossi M, Caruso F. FT-IR spectra of alginic acid blocks fractions in three species of brown seaweeds. *Carbohydr Res.* 2008;343:308–316.
32. Tahermansouri H, Khoei DC, Meskinfam M. Functionalization of carboxylated multi-walled carbon nanotubes with 1,2-phenylenediamine. *Int J Nano Dimension.* 2010;1:153–158.
33. Sarmento B, Ferreira D, Veiga F, Ribeiro A. Characterization of insulin-loaded alginate nanoparticles produced by ionotropic pre-gelation through DSC and FTIR studies. *Carbohydr Polym.* 2006;66:1–7.
34. Swetha M, Sahithi K, Moorthi A, Srinivasan N, Ramasamy K, Selvamurugan N. Biocomposites containing natural polymers and hydroxyapatite for bone tissue engineering. *Int J Biol Macromol.* 2010;47:1–4.
35. Murphy CM, Haugh MG, O'Brien FJ. The effect of mean pore size on cell attachment, proliferation and migration in collagen-glycosaminoglycan scaffolds for bone tissue engineering. *Biomaterials.* 2010;31:461–466.
36. Yang Q, Peng J, Guo Q, et al. A cartilage ECM-derived 3-D porous acellular matrix scaffold for in vivo cartilage tissue engineering with PKH26-labeled chondrogenic bone marrow-derived mesenchymal stem cells. *Biomaterials.* 2008;29:2378–2387.
37. Mandal BB, Kundu SC. Osteogenic and adipogenic differentiation of rat bone marrow cells on non-mulberry and mulberry silk gland fibroin 3D scaffolds. *Biomaterials.* 2009;30:5019–5030.
38. Mygind T, Stiehler M, Baatrup A, et al. Mesenchymal stem cell ingrowth and differentiation on coralline hydroxyapatite scaffolds. *Biomaterials.* 2007;28:1036–1047.
39. Ren L, Tsuru K, Hayakawa S, Osaka A. Novel approach to fabricate porous gelatin-siloxane hybrids for bone tissue engineering. *Biomaterials*. 2002;23:4765–4773.
40. Magnusson P, Larsson L, Magnusson M, Davie MW, Sharp CA. Isoforms of bone alkaline phosphatase: characterization and origin in human trabecular and cortical bone. *J Bone Miner Res.* 1999;14:1926–1933.
41. Li Z, Ramay HR, Hauch KP, Xiao D, Zhang M. Chitosan-alginate hybrid scaffolds for bone tissue engineering. *Biomaterials.* 2005;26:3919–3928.
42. Kim U-J, Park J, Kim HJ, Wada M, Kalpan DL. Three-dimensional aqueous-derived biomaterial scaffolds from silk fibroin. *Biomaterials.* 2005;26:2775–2785.
43. Wu X, Liu Y, Li X, et al. Preparation of aligned porous gelatin scaffolds by unidirectional freeze-drying method. *Acta Biomater.* 2010;6:1167–1177.
44. Shi X, Sitharaman B, Pham QP, et al. Fabrication of porous ultra-short single-walled carbon nanotube nanocomposite scaffolds for bone tissue engineering. *Biomaterials.* 2007;28:4078–4090.